Spectroscopic and Electrochemical Observation of Both 17- and 19-Electron States of an Inorganometallic Transition Metal Complex: $[Fe^{III}(\eta^5\text{-}C_5Me_5)(S_2CNMe_2)_2]$

Marie-Hélène Delville-Desbois,[a] François Varret[b] and Didier Astruc[a]

[a] *Laboratoire de Chimie Organique et Organométallique, URA CNRS No. 35, Université Bordeaux I, 351 Cours de la Libération, 33405 Talence Cédex France*

[b] *Département de Recherches Physique, URA CNRS No. 71, Université Pierre et Marie Curie, Case 136, 4 Place Jussieu, 75252 Paris Cédex 05, France*

The blue 19e complex $[Fe^{III}(C_5Me_5)(\eta^2\text{-}S_2CNMe_2)_2]$ **1**, generated by addition of NaS_2CNMe_2 to the 17e complex $[Fe^{III}(C_5Me_5)(\eta^2\text{-}S_2CNMe_2)(MeCN)]PF_6$ in MeCN at −45 °C or by monoelectronic reduction of the 18e cation **1**$^+$ using the 19e complex $[Fe^I(C_5H_5)(C_6Me_6)]$ in THF at −80 °C gives the purple 17e form $[Fe^{III}(C_5Me_5)(\eta^2\text{-}S_2CNMe_2)\text{-}\{\eta^1\text{-}SC(S)NMe_2\}]$ **2** in solution and in the solid state; both the 17e and 19e forms are characterized by their specific ESR and Mössbauer spectra and by cyclic voltammetry.

Paramagnetic complexes play a major role in redox catalysis and electrocatalysis[1,2] and therefore their structure–reactivity relationship is of crucial interest.[2–4] In particular, their fast, extremely facile 17e ⇄ 19e interconversion stands as a major landmark of paramagnetic transition metal chemistry.[1–4] Recently, we have proposed a 'chameleon'-type behavior of these complexes involving rapid interconversion between the 17, 18 and 19e potential wells.[4] Although the 19e state has been so far almost exclusively spectroscopically characterized in sandwich complexes,[4a] it has been involved as intermediate or transition state in associative ligand-exchange processes of 17e metal carbonyl complexes.[1,4] Trapping experiments have also brought convincing evidence that 19e species must exist.[6a] Finally, ligand-based radicals have been characterized, but they should be considered as 18e (or 18 + δ with $0 < \delta \leq 0.2$) rather than 19e complexes.[3d,6] We wish to report here the spectroscopic and electrochemical observations of both 17e and 19e states for the same molecule. We also use both modes of generation of 19e species: ligand addition to a 17e species (17 + 2) and monoelectronic reduction of a 18e precursor (18 + 1).

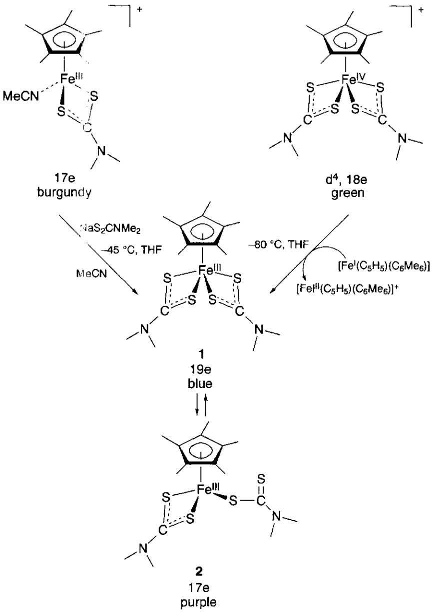

Scheme 1

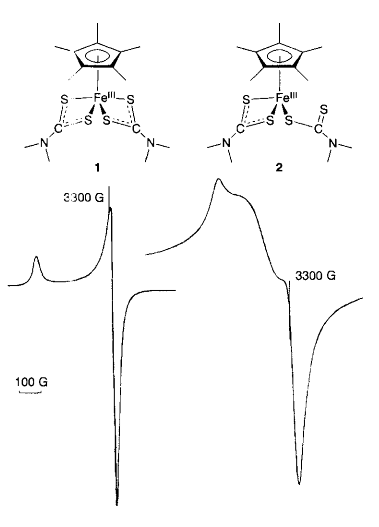

Fig. 1 ESR spectra of **1** and **2** at 20 K (solid-state samples)

The 19e blue complex **1** was generated either by reaction of NaS_2CNMe_2 with the 17e complex $[Fe^{III}(C_5Me_5)(\eta^2\text{-}S_2CNMe_2)(MeCN)]PF_6$[7a] in MeCN at −45 °C or by exergonic electron transfer (ET) between $[Fe^I(C_5H_5)(C_6Me_6)]$ and $1^+PF_6^-$ in THF at −80 °C (Scheme 1). In the solid state, the 19e form **1** is stable at room temperature for 15 d as shown by Mössbauer studies (*vide infra*, Fig. 2). However, in polar solvents such as MeCN, it is stable only up to −40 °C. Above this temperature, in MeCN, the blue complex **1** then leads to the purple 17e form **2** {the neutral iron(II) model $[Fe(C_5Me_5)(\eta^2\text{-}S_2CNMe_2)(SCN)]$ is also purple}.[7b]† When extracted with toluene at −80 °C and separated from $NaPF_6$, the 19e form **1**

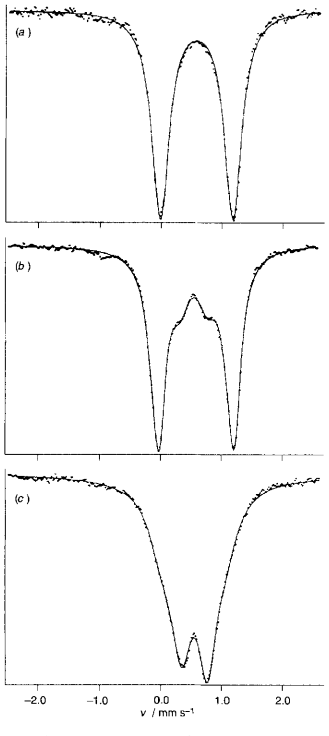

Fig. 2 Iron-57 Mössbauer spectra of **1** recorded at 77 K showing the transformation of complex **1** to **2** with time; (*a*) fresh sample, (*b*) after 6 days at 300 K, (*c*) after 26 days at 300 K

turns out to be stable at 20 °C for several hours. However, solution samples of **1** or **2** synthetized by either route rapidly decomposed at 20 °C under the influence of $NaPF_6$ in MeCN. Indeed, the special salt effect[8,9] can induce a double ion-pair exchange driving the dismutation ET[9] of eqn. (1) ($\Delta G° \approx 33$ kJ mol^{-1}, see the CV, Fig. 3).

$$\mathbf{1} + \mathbf{2} \rightleftarrows [\mathbf{1}^+, \mathbf{2}^-] \xrightleftharpoons{NaPF_6} [\mathbf{1}^+, PF_6^-] + [Na^+, \mathbf{2}^-] \rightarrow \text{decomposition} \quad (1)$$

The ESR spectrum of **1** at 20 K [Fig. 1(*a*)] shows a perfectly axial symmetry with two *g* values ($g_\perp = 2.2751, g_{/\!/} = 2.0289$) which reflect a metal-based SUMO. In contrast, the 17e complexes $[Fe(C_5Me_5)(\eta^2\text{-}S_2CNMe_2)X]$,[7b] such as the model (X = SCN) and **2**, exhibit ESR spectra at 20 K [Fig. 1(*b*)] with characteristic rhombic distortion (three *g* values: $g_1 = 2.2680$, $g_2 = 2.126$, $g_3 = 2.0350$).

The zero-field Mössbauer spectra of **1** also show a single doublet with parameters (IS = 0.54 mm s^{-1} *vs.* Fe, QS = 0.94 mm s^{-1} at 77 K, Fig. 2(*a*)] different from those of the 17e family)[7b] which exhibits a variation of the quadrupole splitting with the temperature which compares to iron(I) complexes (from QS = 0.98 mm s^{-1} at 4.2 K to 0.90 mm s^{-1} at 300K).[3a] The evolution of Mössbauer spectra of **1** upon raising the temperature shows the appearance and increase of a new doublet concomitant with the decrease of the doublet of **1** and having the characteristics of a 17e iron(III) complex (IS = 0.499 mm s^{-1} *vs.* Fe, QS = 0.332 mm s^{-1} at 77 K) [Fig. 2(*c*)].

The overall CV (Fig. 2) of 1^+PF_6- can be divided into the left zone corresponding to the redox processes between cationic and neutral species and the right one which exhibits the redox processes between neutral and anionic complexes. The major chemical reaction following cathodic reduction is the partial decoordination of one S_2CNMe_2 ligand from an η^2 to an η^1 mode. The waves corresponding to redox processes involving η^2 species exhibit decreasing intensity upon repeated scanning (R_1, R_4, O_2, O_5) whereas those involving η^1 species increase (R_0, R_3, O_1,O_4). Finally, a minor observable process is the coordination of η^1 species by a solvent molecule L and the ensuing redox processes of η^1L (R_2 and O_3) with increasing wave intensity. The result is a triple-square scheme (Scheme 2).[10] If only the cationic/neutral redox zone is scanned for several cycles, the waves corresponding to η^2 species (R_1 and O_2) decrease much less than if the potential scan takes in the second couple, indicating that the decoordination rate is much faster at the anionic (20e) level than at the neutral (19e) one. Isopotential peaks are found at −0.20 V on the reductive scan and −0.10, −0.31, −0.40 and −0.83 V when both zones are scanned and indicate that the decoordination of the 20e anion $(\eta^2)^-$ to the 18e anion $(\eta^1)^-$ is quantitative and clean (no side reaction). Indeed, no free $S_2CNMe_2^-$ can be detected by CV in the cell.

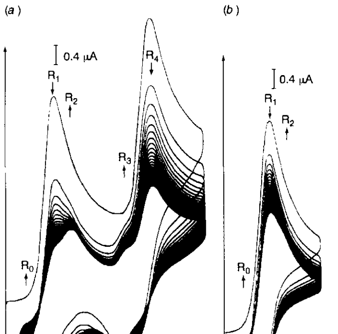

Fig. 3 Cyclic voltammogram under continuous scan of a 2.22×10^{-5} mol dm^{-3} DMF solution of $1^+PF_6^-$ (0.1 mol dm^{-3} $Bu^n{}_4NBF_4$, at Pt electrode, scan rate = 0.6 V s^{-1}, 20 °C; (*a*) switching potential beyond the second electron transfer, (*b*) switching potential between both electron transfers

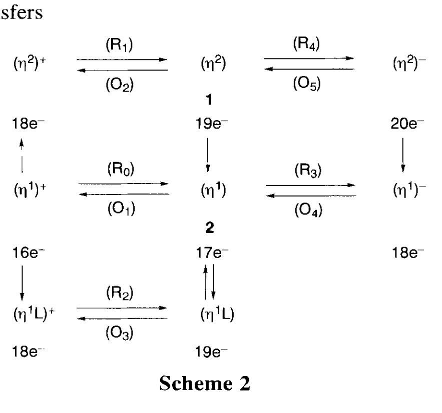

Scheme 2

Thus the macroscopic phenomena can be monitored by CV which reveals decoordination at the 19e and 20e levels. In conclusion, it appears that 19e species can be observed using spectroscopic methods and CV. Their decoordination to 17e complexes can also be characterized.

This work was supported by the Universities Bordeaux I and Paris VI, the CNRS and the Région Aquitaine. We thank the Laboratoire de Chimie du Solide, the Universities Bordeaux I and Paris VI and Dr J. M. Dance (Bordeaux) for ESR facilities and discussions.

Received, 21st October 1994; Com. 4/06463A

Footnote

† Satisfactory elemental analysis was obtained.

References

1 H. Taube, *Angew. Chem., Int. Ed. Engl.*, 1984, **23**, 329; *Paramagnetic Organometallic Species in Activation Selectivity and Catalysis*, ed. M. Chanon, M. Julliard and J. C. Poite, NATO ASI Series, Kluwer Academic, Dordrecht, 1989; M. Tilset, in *Energetics of Organometallic Species*, ed. J. A. Simoes, Kluwer, Dordrecht, 1992, p. 109; D. Astruc, *Angew. Chem.*, 1988, **100**, 662; *Angew. Chem., Int. Ed. Engl.*, 1988, **27**, 643.

2 D. Astruc, *Electron-Transfer and Radical Processes in Transition Metal Chemistry*, VCH, New York, 1995, ch. 6 and 7.

3 (*a*) N. G. Connelly, *Chem. Soc. Rev.*, 1989, **18**, 153; (*b*) W. E. Geiger and N. G. Connelly, *Adv. Organomet. Chem.*, 1985, **24**, 87; (*c*) N. G. Connelly and W. E. Geiger, *Adv. Organomet. Chem.*, 1984, **23**, 1; (*d*) D. R. Tyler, *Prog. Inorg. Chem.*, 1988, **36**, 125.

4 (*a*) D. Astruc, *Chem. Rev.*, 1988, **88**, 1189; *Acc. Chem. Res.*, 1991, **24**, 36; (*b*) J. Ruiz, M. Lacoste and D. Astruc, *J. Am. Chem. Soc.*, 1990, **112**, 5471.

5 A. Poe, *Transition Met. Chem.*, 1982, **7**, 65; see also Ref. 2, ch. 5.

6 D. R. Tyler, *J. Organomet. Chem. Library*, 1990, **22**, 338; D. Fenske, *Angew. Chem.*, 1976, **88**, 415; *Angew. Chem., Int. Ed. Engl.*, 1976, **23**, 381; *Chem. Ber.*, 1979, **112**, 363.

7 (*a*) M.-H. Desbois and D. Astruc, *Angew. Chem.*, 1989, **101**, 460; *Angew. Chem., Int. Ed. Engl.*, 1989, **28**, 459; (*b*) M.-H. Delville-Desbois and D. Astruc, unpublished work.

8 S. Winstein, E. Clippenger, A. Fainberg and G. C. Robinson, *J. Am. Chem. Soc.*, 1954, **76**, 2597; A. Loupy and B. Tchoubar, *Salt Effects in Organic and Organometallic Chemistry*, VCH, Weinheim, 1992.

9 A. Loupy, B. Tchoubar and D. Astruc, *Chem. Rev.*, 1992, **92**, 1141.

10 For organometallic electrochemical mechanisms, see: W. E. Geiger, *Prog. Inorg. Chem.*, 1985, **33**, 275; J. Heinze, *Angew. Chem.*, 1984, **96**, 823; *Angew. Chem., Int. Ed. Engl.*, 1984, **23**, 831; 1993, **105**, 1265; 1993, **32**, 1268; D. H. Evans, *Chem. Rev.*, 1990, **90**, 739.